# Optimal Energy Management System for Storage-Integrated Multi-Energy Microgrids

Ehsan Hosseini, Pablo Horrillo-Quintero, Pablo García-Triviño, Carlos Andrés García-Vázquez, Higinio Sánchez-Sainz and Luis M. Fernández-Ramírez

*Published in:*
24th International Conference on Environment and Electrical Engineering and 8th I&CPS Industrial and Commercial Power Systems Europe (EEEIC24)

*DOI (link to publication from Publisher):*
10.1109/EEEIC/ICPSEurope61470.2024.10751469

*Publication date:*
Not available

*Document Version:*
Accepted version

Citation for published version (IEEE):
Ehsan–Hosseini, P. Horrillo–Quintero, P. García–Triviño, C. Andrés García–Vázquez, H. Sánchez–Sainz and L. M. Fernández–Ramírez, "Optimal Energy Management System for Storage-Integrated Multi-Energy Microgrids," 2024 IEEE International Conference on Environment and Electrical Engineering and 2024 IEEE Industrial and Commercial Power Systems Europe (EEEIC / I&CPS Europe), Rome, Italy, 2024, pp. 01-06, doi: 10.1109/EEEIC/ICPSEurope61470.2024.10751469.

# Optimal Energy Management System for Storage-Integrated Multi-Energy Microgrids


1st Ehsan-Hosseini
*SURET Research Group*
*Department of Electrical Engineering*
*University of Cadiz*
Algeciras, Spain
ehsan.hosseini@uca.es

2nd Pablo Horrillo-Quintero
*SURET Research Group*
*Department of Electrical Engineering*
*University of Cadiz*
Algeciras, Spain
pablo.horrillo@uca.es

3rd Pablo García-Triviño
*SURET Research Group*
*Department of Electrical Engineering*
*University of Cadiz*
Algeciras, Spain
pablo.garcia@uca.es

4th Carlos Andrés García-Vázquez
*SURET Research Group*
*Department of Electrical Engineering*
*University of Cadiz*
Algeciras, Spain
carlosandres.garcia@uca.es

5st Higinio Sánchez-Sainz
*SURET Research Group*
*Department of Electrical Engineering*
*University of Cadiz*
Puerto Real, Spain
higinio.sanchez@uca.es

6th Luis M. Fernández-Ramírez
*SURET Research Group*
*Department of Electrical Engineering*
*University of Cadiz*
Algeciras, Spain
luis.fernandez@uca.es



***Abstract*—The paper describes the design and evaluation of a multi-energy microgrid (MEMG) that incorporates renewable energy sources (RES), battery storage (BS), fuel cells (FC), electrolyzer (ELZ) as hydrogen vector, and thermal vector to meet residential energy demands. The focus of the paper is on developing an optimal energy management system (EMS) using the 'fmincon' optimization algorithm to economically dispatch power between electrical and hydrogen sources while maintaining a balance between thermal and electrical power across all components of the microgrid. The EMS is evaluated using Simulink under different weather scenarios and varying thermal/electrical demands. The results indicate that the proposed EMS effectively controls the power flow from the BS, FC, and ELZ ensuring that minimum costs are imposed on the MEMG while the demands are met under all conditions. Additionally, it suggests that the MEMG is largely self-sufficient, requiring minimal intervention from the grid.**



***Keywords— optimal energy management system, multi-energy microgrids, energy storages, thermal and electrical balances.***


## I. Introduction

The microgrid (MG) adoption with renewable energy sources (RES), particularly incorporating solar energy through photovoltaic (PV) power sources, along with the integration of energy storage systems, represents a sustainable and resilient approach to meeting energy needs [1,2]. This combination not only reduces reliance on traditional and finite resources but also contributes to the transition towards a more environmentally friendly and reliable energy infrastructure [3].

MGs exhibit versatility in their operational modes, and two distinct states are often identified: isolated operation and grid-connected operation [4]. In isolated operation, MGs function independently, generating and utilizing energy within a closed system. The generated energy can be either consumed locally or stored for future use within the MG. On the other hand, in grid-connected MGs, the MG is interconnected with a larger master grid. This connectivity allows for the exchange of power between the MG and the main grid through a common coupling point, enabling a more dynamic and flexible energy management.


This work was partially supported by Ministerio de Ciencia e Innovación, Agencia Estatal de Investigación, and Unión Europea (Grant TED2021-129631B-C32 supported by MCIN/AEI/10.13039/501100011033 and NextGenerationEU/PRTR).


The introduction of small-scale multi-energy microgrids (MEMGs) has been particularly targeted at local industries and residential areas, catering to the diverse energy needs arising from the common usage of both electricity and gas. In contemporary applications, RES like PV systems play a significant role in supplying thermal and electrical energy to MEMGs, supported by a combination of energy storage and gas energy. MEMGs further enhance this flexibility by integrating various types of energy production and consumption, including gas, electricity, and hydrogen (H2) [5]. This composition allows MEMGs to incorporate diverse units, providing adaptability to different energy sources and demands. The configuration of a MEMG is highly adaptable and varies based on the specific application it is designed for. Typically, a MEMG is composed of various interconnected units, each serving a specific function. These units can be categorized as RES, energy storages, conversion systems, transmissions, and demand units [6]. The interconnection of these units within the MEMG allows for a dynamic and responsive energy system that can efficiently balance the fluctuations in energy supply and demand. This adaptability is particularly valuable in accommodating the intermittency of RES and ensuring a reliable and sustainable energy supply for local industries and residential applications.

A novel application of MEMGs is for residential use, where they can include both thermal and electrical components. In the thermal part, various elements such as gas boilers (GB), electrical boilers (EB), underfloor heating (UH), water heating, cooling systems, and other thermal equipment contribute to a comprehensive energy system [7]. The electrical part encompasses residential loads, and notably, electric vehicles (EVs) can be integrated as electrical loads.

The successful coordinated operations, control, and stability assessment of MEMGs rely heavily on accurate and comprehensive modeling of the MG components. To facilitate this, several environments, open-source modelling tools, and toolboxes have been developed. Two notable examples are MESMO [8] and FLEDGE [9], and there is also the CARNOT toolbox [10], specifically designed for Simulink, which includes thermodynamic and energy-engineering models. Achieving efficiency in a MEMG requires a seamless bidirectional collaboration between the thermal and electrical components. Many studies have highlighted the importance of utilizing RES to generate thermal power. This approach aims


979-8-3503-5518-5/24/$31.00 ©2024 IEEE

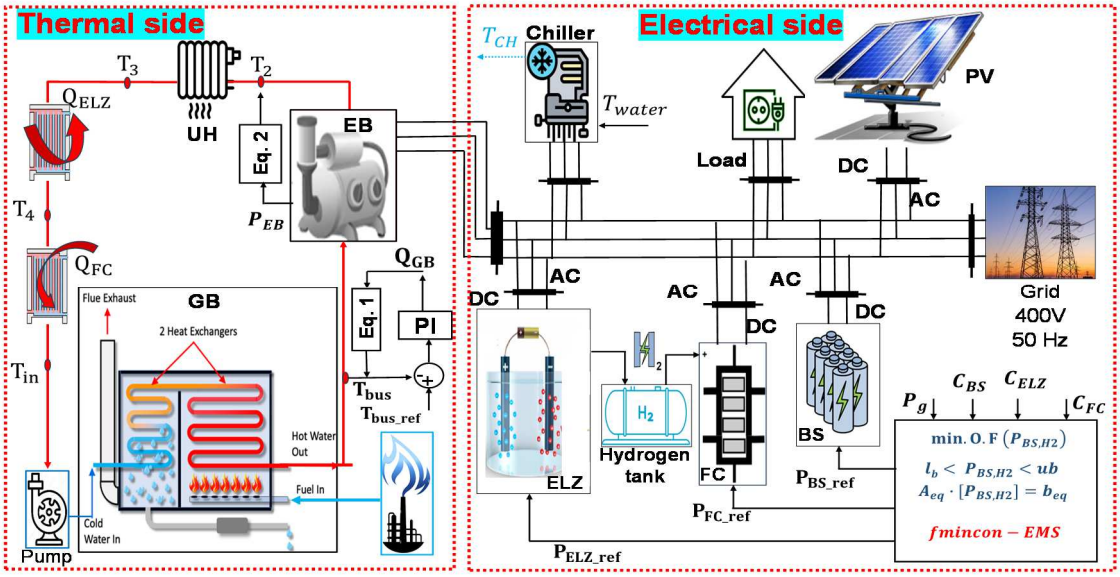


**Fig. 1.** MEMG under study

to reduce dependence on traditional gas-based thermal systems, aligning with the goals of sustainable and environmentally friendly energy systems. Reference [11] collectively highlighted the necessity of advanced optimization methods and dynamic modeling techniques to enhance the performance of MEMGs. There is a dearth of research like [12, 13] that delves into dynamic modeling and control of MEMGs in RES-based systems. By dynamically adapting to fluctuations in RESs and integrating surplus energy for heating demands, these approaches contribute to improving the reliability, efficiency, and overall performance of RESs. Coordinated control methods further enhance the adaptability of the system, allowing it to respond effectively to changing conditions and demands.

Reference [14] modelled a MEMG with combined heat and power, and thermal energy storage and examined the operational principles of ground source heat pumps (GSHP). Although this paper addressed the long-term impacts of cross-seasonal heat balance on the GSHP coefficient of performance and lifespan, the system was modelled statically in Python in a gentle RES output power. The mentioned model lacked a practical assessment of thermal elements and environmental behaviour. While reference [15] investigated the optimal operation of MEMG elements is in buildings with PV, integrated demand response and heterogeneous energy storage, it relied on steady-state analysis. A multi-time scale optimization strategy is necessary to account for varying response characteristics and dynamic changes across diverse energy sources. Moreover, this work did not explore a participation degree model for energy consumers engaging in integrated demand response, considering the influence of both electricity and natural gas prices.

Most previous studies either rely on statistical models with short-term evaluations or focus on dynamic models that prioritize power balancing without considering the economic cost of utilizing different elements. This paper suggests an opportunity for future research to bridge this gap by developing comprehensive models that not only address dynamic behaviour and practical assessments but also provide economic control strategies for MEMGs. In this paper, an economical evaluation of a MEMG is conducted through a nearly quarter-day simulation under varying power production and consumption. An economically driven EMS is designed, utilizing MATLAB 'fmincon' optimizer to control the proposed MEMG, which integrates electrical and thermal components. Through ELZ and FC, electrical energy is converted to H2 and stored in an H2 tank. This stored H2 can be reconverted to electricity when demand peaks, providing additional support to the system alongside the PV power production and BS to feed household loads. CARNOT Toolbox is used to design the thermal components and buses within the MEMG.

The remainder of this paper is organized as follows. Section 2 provides readers with a comprehensive understanding of the MEMG with the coordination between the thermal and electrical aspects as well as the thermal load elements. Section 3 presents the fmincon-based EMS for the proposed MEMG. Section 4 evaluates the proposed EMS by simulation results. Finally, Section 5 wraps up the paper by briefly revisiting the key points discussed throughout the paper.

## II. SYSTEM UNDER STUDY

A MEMG is designed to connect to a three-phase 400V grid and includes various components including electrical, thermal, and H2 vectors, as shown in Fig. 1. The electrical vector includes an 18-kW PV power plant for generating electricity, a 26.6-kWh BS system with a nominal voltage of 345V for storing excess energy, and household electrical load representing the energy consumption of the connected load. Regarding H2 vector, a 20-kW ELZ is utilized to convert excess electrical energy into H2. A 1000g tank is specifically designed to store the generated H2, while a 10-kW FC is activated when the MEMG requires additional power, converting the stored H2 back into electrical energy. The thermal vector includes a GB used for heating water, an EB with a heating capacity of 23-kW a water storage capacity of 300 liters, a varying UH, and a 15-kW cooling chiller.

Given the intermittent nature of RES, continuous energy utilization over a 24-hour period becomes challenging. To address this issue, storage systems are essential. Additionally, considering the substantial demand for power from both electrical and thermal loads in this scenario, a BS system and

a H2 tank with sufficient capacities are integrated into the proposed MEMG. During periods when the MEMG experiences insufficient PV power, the BS and FC are activated to supplement energy production and meet the load demands. Conversely, when the generated power exceeds the load requirements, surplus energy can be stored in the BS or converted into H2 energy and stored in the H2 tank. This stored energy can then be utilized during periods of low PV production to ensure continuous power supply.

To integrate thermal aspects into the simulation, the CARNOT toolbox was introduced to the Simulink library, enabling dynamic modeling. However, certain process control constraints such as delay times, burner initialization, and the combustion process were omitted in this study. The system treats water as a heat carrier circulating through various thermal elements. A multi-node model was utilized on the water-side of the furnace within the combustion chamber of the boiler. This approach allows for the generation of hot water by circulating cold water through a heat exchanger. The model incorporates a condensing boiler equipped with two heating exchangers, facilitating the transfer of heat between the water and the burning fuel.

In addition to the boiler, another component utilized for heating water is the EB, which consumes electrical energy. The water mass flow introduced into the EB is warmed by the power supplied by the electrical side of the MEMG. In the design of the EB, insulation layers were incorporated to reduce energy consumption and minimize heat dissipation. Additionally, a thermal node was defined in the model to factor in ambient thermal losses. This comprehensive approach ensures efficient heating while considering insulation and ambient conditions to optimize energy usage within the system.

In the proposed thermal system, the circulation of water between components is outlined as follows: Initially, electrical pumps are employed to pressurize water within the building supply pipes, facilitating its entry into the GB. Within the GB, the water is heated utilizing its heat exchangers. To further elevate the water temperature, an EB is incorporated and connected to the GB via a thermal bus. The EB is powered by the electrical side of the MEMG. The temperature of the thermal bus ($T_{bus}$) must align with specific thermal load requirements, such as those for hot water and underfloor heating. To achieve this, a PI controller is utilized to adjust the temperature, minimizing the disparity between the GB and the thermal bus. This approach ensures effective temperature regulation within the thermal system to meet diverse heating demands efficiently.

## III. Energy Management System (EMS)

This paper proposes an EMS for the MEMG, with the goal of optimizing the use of BS, ELZ, and FC components. This EMS sets specific powers and temperatures based on system operation. Based on the gap between production, consumption and available storage energy, the EB power, thermal bus temperature, and EB turn-off temperature ($T_{EB}^{max}$), are determined. Developing dynamic models for the GB and EB output temperatures requires considering various factors based on energy balance and the first law of thermodynamics. These include heat input, heat losses, boiler efficiency, and system thermal properties. Here, we explain the formulation of such a dynamic model [16]:

$$\left(m \cdot c \cdot \frac{1}{N}\right) \cdot \frac{dT_{bus}}{dt} = \left(UA \cdot \frac{1}{N}\right) \cdot (T_{amb} - T_{bus}) + (\dot{m}_{bus} \cdot c_f) \cdot (T_{in} - T_{bus}) + Q_{GB} \quad (1)$$

$$C_{EB} \cdot \frac{dT_{EB}}{dt} = UA \cdot (T_{amb} - T_{EB}) + (\dot{m}_{water} \cdot c_p) \cdot (T_{bus} - T_{EB}) + P_{EB} \quad (2)$$

where, $m$ is the mass of water in the EB, c is the heat capacity, $N$ is the number of nodes, $UA$ is the heat loss coefficient to ambient, $T_{amb}$ is the ambient temperature, $c_f$ is the heat capacity of fluid, $T_{in}$ is the temperature of fluid at the input, $C_{EB}$ is the thermal capacity of the boiler, and $c_p$ is the heat capacity of fluid.

To model an absorption chiller, it relies on characteristic curves and the coefficient of performance (COP) of a real chiller unit. By incorporating characteristic curves, COP data, and waste heat recovery principles into the modeling approach, it can effectively simulate the performance of an absorption chiller and understand its behavior under different operating conditions. This understanding is crucial for optimizing the chiller's performance and maximizing energy efficiency in practical applications [17].

The control objective focuses on reducing utilization costs of storages by optimizing the utilization of these components, while also considering factors such as BS, ELZ, and FC durability. An objective function (OF) is formulated based on utilization cost reduction, considering factors such as electricity prices and component degradation costs. The optimization problem is solved using a constrained nonlinear multivariable function solver, referred to as '*fmincon*'. This solver is utilized to find the optimal allocation of power among the electrical and *H2* components while satisfying the imposed constraints. The proposed objective function, which is based on cost minimization, is formulated as follows:

$$O.F. = C_{BS} \,.\, P_{BS} + C_{ELZ} \,.\, P_{Elz} + C_{FC} \,.\, P_{FC} \quad (3)$$

Constraints are imposed on the optimization problem to ensure feasibility and safety. These constraints include the state-of-the-charge (SOC) limit of the BS, H2 tank level, maximum power capacities of the components (BS, ELZ, FC), and available power, the difference between generated power and demanded one, that must be dispatched between electrical and H2 parts. These constraints are discussed in the following subsections.

### A. Power Equality

The optimization algorithm prioritizes meeting demand during renewable energy shortfalls by strategically utilizing storage systems. Conversely, when renewable energy exceeds demand, it prioritizes storing excess energy for later use. To include these conditions in the optimization process, a linear equality constraint (power equality constraint) is defined in the optimization process to share the power among storages. This equality constraint is applied to the *'fmincon'* algorithm by considering two equality factors, denoted as $A_{eq}$ and $b_{eq}$ ($A_{eq} \cdot [P_{BS+H2}] = b_{eq}$). As three components are proposed in this work, and the BS ans FC must support the RES production to provide a balanced power, then $A_{eq} = [1\ 1\ 1]$, and $b_{eq}$ is considered as the difference between the gap power (difference between the RES production power and the

electrical power demanded by the loads) and the power requested by the EB.

$$P_{gap} = P_{RES} - P_{loads} \quad (4)$$

$$P_s = P_{gap} - P_{EB} \quad (5)$$

$$b_{eq} = P_s \quad (6)$$

### B. Power Bounds

Power limitations are considered for BS and H2 components for the optimization constraints. The maximum powers that each of them can produce or receive are calculated by the following expressions [9]:

$$P_{ELZ}^{max} = \min\left(P_{ELZ}^{nom}, B \cdot Q_{H2}^{nom} + A \cdot \frac{M_{H2}^{nom}}{\Delta t} \cdot \frac{100 - L_{H2}}{100}\right) \quad (7)$$

$$P_{FC}^{max} = \min\left(P_{FC}^{nom}, \eta_{therm} \cdot U_f \cdot \eta_{stack} \cdot \frac{E_{H2}^{nom}}{\Delta t} \cdot \frac{L_{H2}}{100}\right) \quad (8)$$

$$P_{BS,ch}^{max} = min\left(P_{BS}^{nom}, \frac{E_{BS}^{nom}}{\Delta t} \cdot \left(\frac{100 - SOC_{BS}}{100}\right)\right) \quad (9)$$

$$P_{BS,dis}^{max} = min\left(P_{BS}^{nom}, \frac{E_{BS}^{nom}}{\Delta t} \cdot \left(\frac{SOC_{BS}^{min} - SOC_{BS}}{100}\right)\right) \quad (10)$$

where $A$ and $B$ are the ELZ constants, $Q_{H2}^{nom}$ is the nominal hydrogen flow of the ELZ, $M_{H2}^{nom}$ denotes the H2 tank capacity, $L_{H2}$ is the H2 tank level, $\eta_{therm}$ is the fuel cell thermodynamic efficiency, $U_f$ is the FC utilization factor, $\eta_{stack}$ is the FC stack efficiency, $E_{BS}^{nom}$ is the nominal energy of the BS and $SOC_{BS}^{min}$ is the minimum value of the SOC that the BS could have.

The BS power limitation terms in Eqs. (9) and (10) [1] introduce a safety for the SOC value and maintain the charging/discharging power in a range that cares about the BS lifespan.

During the charging mode, the BS output power must be set in the interval $[-P_{BS,ch}^{max}, 0]$, whereas, during discharging mode, these bounds must be in the interval of $[0, P_{BS,dis}^{max}]$.

The same scenario is considered for ELZ as $[-P_{ELZ}^{max}, 0]$, and for FC as $[0, P_{FC}^{max}]$. The EMS produces BS and H2 components power with the above maximum restrictions.

## IV. Simulation Results

In the validation process, the proposed *fmincon*-based EMS for the MEMG undergoes scrutiny through simulation results. A 16000-second simulation is conducted, encompassing a variant thermal/electric pattern in both source and demand, as shown in Fig. 2.

The simulation accounts for fluctuating solar radiation on the source side, while the load side sees variability in parameters such as hot water mass flow, UH demand, and household electrical demands. This rigorous testing aims to assess the effectiveness and robustness of the *fmincon*-based EMS in managing the MEMG under diverse operating conditions. The initial percentages of the H2 level and BS SOC were set to 50 % and 80%, respectively. The PV power plant starts with 17.95-kW power generation, and its production is reduced along with the simulation. The household electrical load gently requests power until 9000th second and after that asks for 5-kW to 20-kW power.

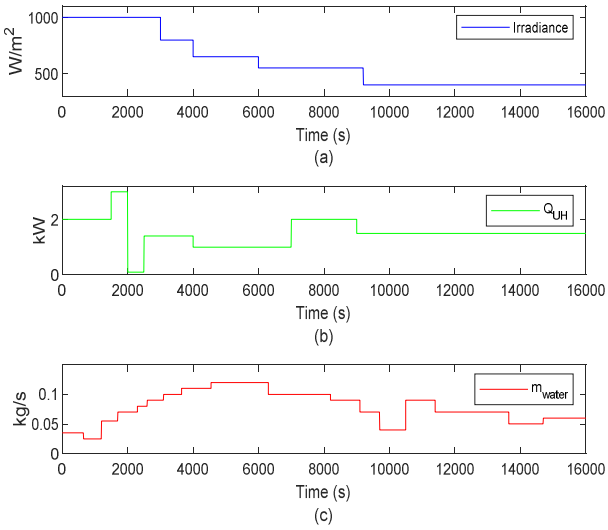


**Fig. 2**. MEMG operating parameters: (a) PV irradiance, (b) underfloor heating demand, and (c) water demand.

Fig. 3 depicts the electrical power balance between the source output power and the load power consumption within the MEMG system. It highlights instances where the electrical balance is maintained, as well as scenarios where adjustments are made to meet demands. Specifically, the graph illustrates that when the EB activates and RES cannot fully meet the electrical demands, the backup system, BS and FC come into play to supplement the power supply. Prior to the 9000-second mark, during periods of high-power production and relatively low household demand, any surplus power generated is utilized to charge the BS and elevate the H2 level ($L_{H2}$) in the tank via the ELZ. However, after the 9000-second mark, when the BS begins discharging and the EB is in operation, the backup system starts discharging as well. During this phase, the FC output power varies between 0 and 20-kW, dependent upon decisions made by the EMS. These variations in power output from the FC are in response to the fluctuating demands of the MEMG system. It is clearly seen that the grid power is zero along with the simulation.

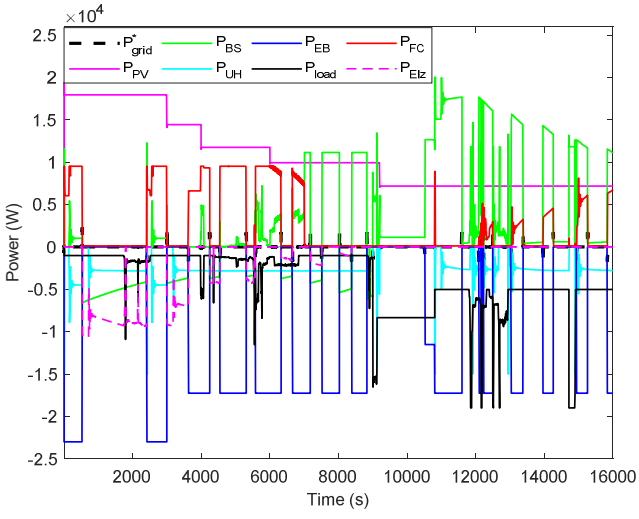


**Fig. 3.** Electrical power productions and consumptions.

Fig. 4 presents the storage state for both the BS and the H2 tank within the MEMG system. Regarding the BS, its charge level fluctuates as it is dynamically charged and discharged in response to the varying requirements of the MEMG. When there is surplus energy available or when the system demands additional power, the BS is charged accordingly. Conversely, when the system requires additional power beyond what is currently being generated, the BS discharges to meet the demand and maintain system stability.

Regarding the H2 tank ( $L_{H2}$ ) is influenced by the operation of the ELZ and the FC within the MEMG. When the ELZ is active, it generates H2 through the electrolysis of water, resulting in an increase in the H2 tank level. Conversely, when the FC is operating, it consumes H2 from the tank to produce electricity, leading to a decrease in the H2 tank level over time. This cyclic behaviour reflects the continuous process of H2 generation and consumption within the MEMG system.

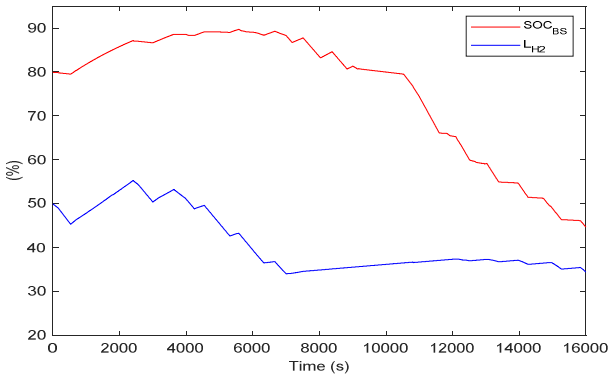


**Fig. 4**. BS SOC and H2 tank level.

In Fig. 5, the thermal powers are depicted, illustrating the necessity for heat production to match heat consumption within the MEMG system. Fig. 5(a) serves to justify the thermal balancing within the system, where the heat generated by GB, FC, and ELZ is equal to the heat consumed by EB and UH. This equality confirms that the MEMG is effectively balancing heat production and consumption, ensuring efficient utilization of thermal energy resources within the MEMG. Fig. 5(b) shows the heat of the EB and its heat in the thermal bus. Depending on the consumer need, the EB works at variable heat levels, ranging from zero to tis maximum potential. However, the bus heat fluctuates within a specific range depending on the heat circulation throughout the thermal part.

Fig. 6 presents the temperatures of various nodes within the MEMG system, including $T_{bus}$ (thermal bus), $T_2$ (EB), $T_3$ (underfloor heating system), $T_4$ (electrolyzer), and $T_5$ (fuel cell). As previously mentioned, these temperatures follow a hierarchy based on heat production or consumption, with $T_{bus} > T_2 > T_3$, $T_{bus} > T_{in} > T_4$. Specifically, $T_{bus}$ represents the temperature of the thermal bus, which tends to be higher than the temperatures of other nodes due to its role in distributing heat throughout the system. $T_2$ represents the temperature of the EB, which typically follows $T_{bus}$ but may exhibit fluctuations depending on thermal activities and losses. $T_3$ corresponds to the temperature of the UH system, which generally lags behind $T_2$ as it consumes heat to raise the water temperature in the pipes for heating purposes. $T_4$ represents

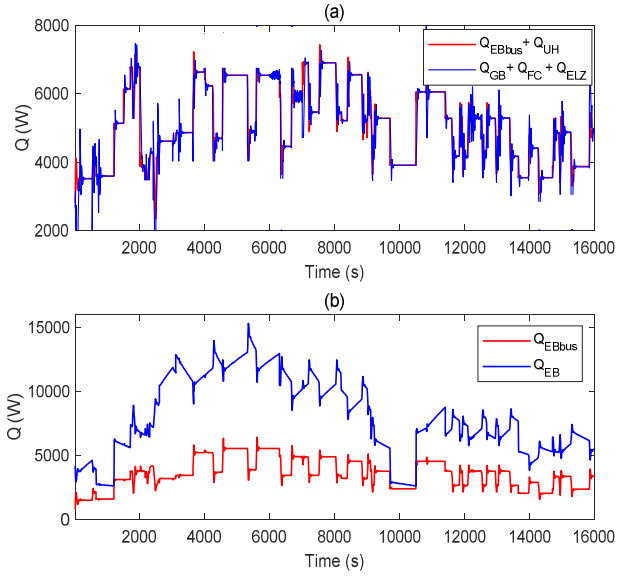


**Fig. 5.** Heat exchanges: (a) heat balance, (b) EB heat, and EB-bus heat.

the temperature of the ELZ, which may vary based on its operational state and the electrolysis process. $T_5$ corresponds to the temperature of the FC, which typically exhibits the lowest temperature among the nodes due to the heat generation associated with its operation. The variation of $T_{bus}$ between 23° to 26° indicates dynamic thermal conditions within the system, with fluctuations occurring during heat exchanges with the environment and among thermal elements. These temperature variations reflect the dynamic nature of the MEMG system, and the continuous adjustments made to maintain thermal balance and system stability.

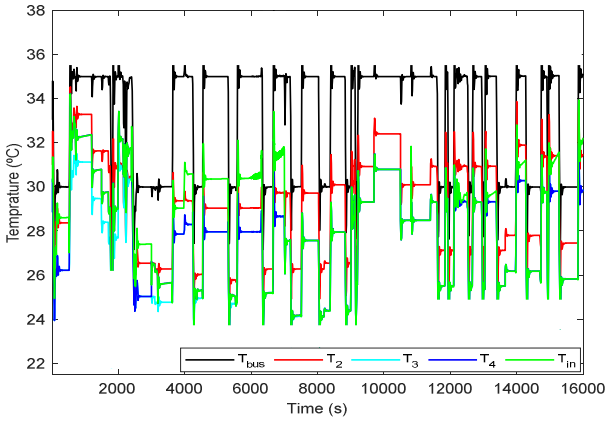


**Fig. 6.** Output temperatures of the thermal nodes.

In Fig. 7, the temperatures of the GB the EB, and the chiller throughout the entire 16000-second simulation are depicted. The temperature of the EB is particularly crucial as it directly influences the hot water supply, typically used for showers and other domestic purposes. Therefore, it is essential for the EB output temperature to remain within a specific range to ensure the availability of hot water. In this simulation, the EB output temperature fluctuates between 50°C and 60°C, indicating that it consistently maintains the desired temperature range throughout the simulation period. Additionally, the performance of the PI controller responsible for adjusting the temperature of the GB is highlighted. The PI controller effectively maintains the thermal bus temperature

($T_{bus}$) at the reference value, ensuring that the overall thermal balance within the MEMG is maintained. This demonstrates the efficacy of the control mechanism in regulating the GB temperature to meet the system requirements and maintain operational stability.

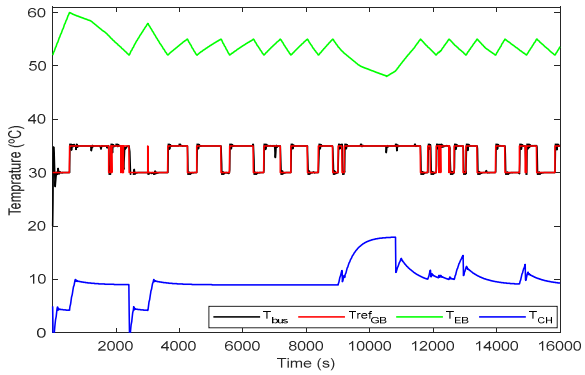


**Fig. 7.** Temperature tracking of the thermal components.

Fig. 8 represents the total costs obtained from the proposed OF. The figure illustrates that as the storage elements generate or store more power, the total operation cost increases. The obtained results prove that the *fmincon*-based EMS effectively manages power dispatch between BS and H2. It prioritizes minimizing the utilization cost of these storage devices while ensuring that generated power levels remain within the safe operating ranges of the components and stored energy capacities. Moreover, the EMS successfully achieves its thermal objectives by maintaining the bus temperature within the desired limits, using ELZ and FC waste heat for water heating circulation, and ensuring a thermal balance between heat production and consumption.

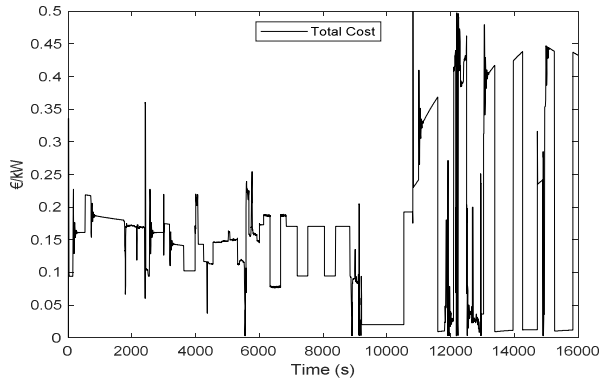


**Fig. 8.** Total operation cost of BS, FC, and ELZ.

## V. Conclusions

This paper has proposed a MEMG designed to meet residential energy needs, including EB operation and household loads. It incorporated BS and H2 sources (FC and ELZ) for flexibility, while also integrating a GB to enable comprehensive evaluation of the entire thermal system, from GB to EB and even an UH system. Achieving economic power dispatch among diverse energy sources like BS, ELZ, and FC was a key focus. The MEMG was evaluated by simulations across various weather conditions and thermal and electrical demands. The evaluation results confirmed the effectiveness of the proposed EMS in managing storage utilization economically and fulfilling energy demands under varied operating conditions. Notably, the EMS achieved these goals while minimizing interventions in grid power, showcasing its ability to maintain grid stability and reduce reliance on external energy sources. Overall, the findings demonstrated the viability and efficiency of the proposed MEMG for residential energy management.

## References


[1] E. Hosseini, P. Horrillo-Quintero, P. García-Triviño, R. Sarrias-Mena, C. Andrés García-Vázquez, and L. M. Fernández-Ramírez "A Nonlinear Programming Solver based on Battery Efficiency Maximization for Quasi-Z-source Cascaded H-bridge Multilevel Inverter with PV and Battery," 4th International Conference on Smart Power & Internet Energy Systems (ONCON), India, 2022.

[2] P. Horrillo-Quintero, et al, "Control System for Quasi-Z-source Cascaded H-bridge Multilevel Inverter with PV Power Generation and Battery Energy Storage System", Proc. of the Interdisciplinary Conference on Mechanics, Computers and Electrics (ICMECE 2022) 6-7 October 2022, Barcelona, Spain.

[3] E. Hosseini, P. García-Triviño, R. Sarrias-Mena, C. Andrés García-Vázquez, and L. M. Fernández-Ramírez "Reinforcement Learning based Energy Management System for Grid-Connected PV plants and Energy-Stored Quasi-Z-source Cascaded H-Bridge Multilevel Inverter," 2023 IEEE International Conference on Environment and Electrical Engineering (EEEIC/I&CPS Europe), Madrid, 2023.

[4] F. Khavari, A. Badri, A.Zangeneh, "Energy management in multi-microgrids considering point of common coupling constraint," International Journal of Electrical Power & Energy Systems, Vol. 115, Feb. 2020.

[5] X. Fang, W. Dong, Y. Wang, Q. Yang, "Multiple time-scale energy management strategy for a hydrogen-based multi-energy microgrid, " Applied Energy, Vol. 328, Dec. 2022,

[6] M. A. Babaei, S. Hasanzadeh, H. Karimi, "Cooperative energy scheduling of interconnected microgrid system considering renewable energy resources and electric vehicles," Electric Power Systems Research,Vol. 229, Apr. 2024.

[7] J. Liu, K. Zeng, H. Wang, B. Lin, B. Du and C. Hu, "Coordinated Operation of An Islanded Multi-energy Microgrid with Demand Response," 2020 IEEE 4th Conference on Energy Internet and Energy System Integration (EI2), Wuhan, China, 2020, pp. 433-438.

[8] V. Kleinschmidt, T. Hamacher and V. Perić, "Flexibility in active distribution networks - modelling a fully coupled multi-energy system in MESMO," 2022 IEEE ISGT Asia, Singapore, pp. 475-479, 2022.

[9] V. Kleinschmidt, S. Troitzsch, T. Hamacher, V. Perić, "Flexibility in distribution systems: Modelling a thermal-electric multi-energy system in FLEDGE," 2021 IEEE ISGT Europe, Espoo, Finland, pp. 1-5, 2021.

[10] S. Lohmann, "FH D E 2 Einführung in die Software MATLAB - Simulink und die Toolboxen CARNOT und Stateflow", 2013.

[11] M. Heleno and Z. Ren, "Multi-Energy Microgrid Planning Considering Heat Flow Dynamics," IEEE Transactions on Energy Conversion, vol. 36, no. 3, pp. 1962–1971, 2021.

[12] X. Lei, Y. Lin, Q. Yang, J. Zhou, X. Chen, and J. Wen, "Research on coordinated control of renewable-energy-based Heat-Power station system," Appl Energy, vol. 324, no. July, p. 119736, 2022.

[13] 15. Z. Li, J. Zhou, J. Wen, and X. Chen, "Dynamic Modeling and Operations of a Heat-power Station System Based on Renewable Energy," CSEE Journal of Power and Energy Systems, vol. 8, no. 4, pp. 1110–1121, 2022.

[14] J. Qi, X. Yan, Q. Liu, W. Yong, L. Xue, X. Yang "Economic dispatch and flexibility enhancement of multi-energy microgrid considering cross-seasonal heat balance of ground source heat pump", Energy Reports, vol. 9, no. 7, pp. 358-369, Sep. 2023.

[15] J. Wang, Ke-J. Li, Y. Liang, J. Zahid, "Optimization of Multi-Energy Microgrid Operation in the Presence of PV, Heterogeneous Energy Storage and Integrated Demand Response", Applied scince, vol. 11, no. 3, pp. 1-19, Jan. 2021.

[16] G. Salvadori, L. Ferrari, L. Romano and F. Fantozzi, "Use of CARNOT Toolbox to Evaluate the Impact of Building Automation and Control Systems on Energy and CO2 Emission Savings," 2020 IEEE International Conference on Environment and Electrical Engineering, Madrid, Spain, 2020, pp. 1-6.

[17] P. Heizen, K. D. Wärmepumpen,"PHB_WP_Heizen_Kuehlen_ES" [Online].Available: www.dimplex.de.